# BAND STRUCTURE ANALYSIS OF 2D PHOTONIC CRYSTALS BY COUPLED-WAVE METHOD: A ROBUST *R*-ALGORITHM

**V.M. FITIO, YA.V. BOBITSKI**[1]

**Lviv Polytechnic National University**
*(12, Stepan Bandera Str., Lviv 79013, Ukraine; e-mail: polyana@polynet.lviv.ua),*

[1]**Institute of Technology, University of Rzeszow**
*(16, T. Rejtan Str., Rzeszow 35-959, Poland)*

UDC 539.2: 537.86


The coupled-wave method (CWM), which is used for the analysis of electromagnetic wave diffraction at planar 1D gratings, has been demonstrated to be able to quickly determine whether the propagation of an electromagnetic wave with an intended frequency is allowed in a 2D photonic crystal, provided that periodic boundary conditions are imposed. The problem is reduced to the solution of the equation $\mathbf{W_1 X} = \rho \mathbf{W_2 X}$ and the verification of whether $|\rho| = 1$. If so, the propagation of the intended frequency is allowed. The dimension of the vector $\mathbf{X}$ is equal to $2N$ – two times the number of the coupled waves used at calculations – and is determined by an accuracy needed for analysis. Since the dielectric constants of typical photonic crystals are characterized by a symmetric spatial dependence, the symmetry considerations allow the dimension of the vector $\mathbf{X}$ to be reduced to $N \pm 1$ or $N$, depending on the symmetry type. In so doing, the calculation time becomes about 8 times shorter, without any loss of resulting accuracy. A modified, robust $R$-algorithm has been used for the numerical analysis.

## 1. Introduction

Intensive researches of photonic crystals, which become the basis for the development of optoelectronic devices of a new type, have been carried out lately. Most of those works were devoted to two-dimensional (2D) photonic crystals [1]. According to work [1], the relative numbers of published works dealing with 3D, 1D, and 2D photonic crystals equal 2, 15, and more than 80%, respectively. Such a statistical distribution may probably be associated with the fact that 1D photonic crystals are the most simple ones for fabrication and there exist accurate methods of their analysis. 1D photonic crystals have been used for rather a long time, even before the term "photonic crystals" has been introduced [2, 3]; nevertheless, they have not exhausted their potential. 3D photonic crystals are the most difficult for the analysis, and there is no reliable technology of their fabrication with controlled defects in the spatial structure of the crystal. From this point of view, 2D photonic crystals occupy an intermediate position: the available method of plane waves [4], although demanding a significant time of computation, provides the accuracy necessary for the analysis of photonic structures; and there are techniques for fabricating such crystals. Therefore, scientific works in this domain are mainly devoted to the properties of 2D photonic crystals and to the development of devices of a new type on their basis [1, 5, 6].

High interest in photonic crystals has been started by E. Yablonovitch's works [2, 3]; the terms "a photonic crystal" and "a photonic band structure" have been introduced at the same time. Nevertheless, it should be noted that it was 3D periodic structures on the basis of a dielectric medium that were proposed for the first time and studied by N.A. Khizhnyak as early as in 1957 [7]. The scientist called such structures artificial anisotropic insulators [7–9]. They were demonstrated to be characterized by a negative effective dielectric constant (or a negative effective magnetic constant in the case of a spatially modulated magnetic insulator) in a certain range of frequencies [8], i.e. – in modern terminology – this frequency range falls within a photonic energy gap. In works [7–9], to analyze the properties of artificial anisotropic insulators, the method of Green's functions was used, which is also applied to the analysis of photonic crystals [10].

For the analysis of the properties of photonic crystals, the plane-wave method [4] is mostly used, where an electromagnetic field in a crystal is considered as a sum of plane waves, and the allowed frequencies are determined as the eigenvalues of a square $2N^d \times 2N^d$-matrix, where $N$ is the number of plane waves used in one direction, and $d$ is the dimensionality of the photonic crystal [11]. Even in the case of a 2D photonic crystal, at least 529 plane waves ($N = 23$) have to be taken into account in order to obtain a desired accuracy [12], i.e. one has to determine the eigenvalues of a $1058 \times 1058$ matrix. For 3D photonic crystals, the problem evidently

becomes even more difficult and demands a large time for computation; moreover, there appears the problem of result convergence [13]. It should be noticed as well that, in the plane-wave method, the allowed frequencies are determined at a given wave vector **k**. In practice, a somewhat different problem arises often enough, namely, to determine whether a given frequency (for instance, a lasing one) is allowed or forbidden to propagate in a 2D photonic crystal, provided that one component of the wave vector is fixed.

Therefore, to analyze 2D photonic crystals quickly, the CWM was proposed [11] which is usually applied to the analysis of 1D diffraction gratings. In this method, a 2D photonic crystal is considered as a stack of gratings, with the thickness of every grating being equal to the period of a photonic crystal in one of the directions. Such a grating system was placed in a homogeneous environment. The CWM was used to calculate the coefficients of transmission through and reflection from the stack of gratings, as well as their dependences on the wavelength. The magnitude of the reflection (transmission) coefficient makes it possible to judge the character of propagation of an electromagnetic wave with a given frequency. However, in any case, this method demands a substantial time for computation, because it is necessary to find a solution in the interval of more than 10 periods. Nevertheless, a comparison between the classical method of calculation of the band structure and the method expounded in work [11], as well as the use of periodic boundary conditions [4], allows a conclusion to be drawn that it is sufficient to obtain the CWM solution in a single period of the photonic crystal only, in order to determine whether the given frequency is allowed or forbidden at all. That is, a method can be formulated to calculate the band structure of a photonic crystal quickly and with a high accuracy. This method was presented in work [14] for the first time. Essentially, it is reduced to a problem of matrix algebra of the type $\mathbf{TX} = \rho\mathbf{RX}$ concerning eigenvalues and eigenvectors. The square matrices **T** and **R** were determined within a single period of the structure in the framework of the CWM and following a robust S-algorithm [15]. The dimension of square matrices was equal to $2N \times 2N$, where $N$ is the number of coupled waves taken into consideration. It is clear that the accuracy and the time of computations increase with increase in $N$. This method was used to construct the band structure of photonic crystals with the simplest square elementary cell and made up of rods with square cross-sections. It means that this method was verified for elementary photonic crystals, but there are no instructions on how it can be used for 2D photonic crystals with a triangular cell. In addition, the method of work [14] does not take the spatial symmetry of photonic crystals [16] into account, although the CWM makes it possible to use the spatial symmetry of the grating and diffraction and to reduce the body of computations by a factor of 4 to 8 without any loss of accuracy [17]. At the same time, in work [14], a robust numerical $S$-algorithm was used for computations, which is rather cumbersome when being applied to 2D photonic crystals composed of rods with non-square cross-sections.

Hence, this work aims at improving the CWM to analyze the band structure of 2D photonic crystals, studying the features of its application, and demonstrating that the advanced method – by its universality – does not concede the classical plane-wave method. At the same time, the improved method is advantageous, because, in the course of computations, one has to operate with matrices, which include a many less number of elements, and this circumstance becomes inevitably reflected in the accuracy and the time of computations.

## 2. Coupled-wave Method

Let us briefly describe the CWM and present the corresponding systems of differential equations for the diffraction of waves with TE- and TM-polarization; in so doing, we will mainly base on works [14,15,18,19]. In the framework of our researches, the wave vector **k**, which describes the wave propagation in a 2D photonic crystal, is supposed to lie in a plane that is perpendicular to the parallel axes of cylinders the crystal is made up of. If the vector of the electric field strength is parallel to the cylinder axes, we deal with waves of TE-polarization; if the vector of the magnetic field is parallel to the cylinder axes, such waves will be referred to as TM-polarized. In Fig. 1, the scheme of a 2D photonic crystal with an $a \times a$-square elementary cell, which is made up of cylindrical rods as an infinite stack of gratings of thickness $a$ each, arranged normally to the $oz$-axis, is presented. The gratings are periodic along the $ox$-axis with the period $\Lambda = a$. The relative dielectric constant of the rods equals $\varepsilon_a$, and that of a surrounding material $\varepsilon_b$.

Consider a grating in the photonic crystal confined by two planes, $z = -a/2$ and $z = a/2$, and thus having the thickness $a$ in the direction of the $oz$-axis. First, we examine the case of TE-polarization. The corresponding

equations look like [14, 15, 18]

$$\frac{dG_n(z)}{dz} = -ik_0 F_n(z), \tag{1}$$

$$\frac{dF_n(z)}{dz} = i\frac{k_{nx}^2}{k_0} G_n(z) - ik_0 \sum_p \|\varepsilon\|_{n-p} G_p(z), \tag{2}$$

where $G_n(z)$ is the electric field strength of the coupled wave characterized by the index $n$, $F_n(z)$ the strength of the tangential component of the magnetic field of the coupled wave with the index $n$, $k_0 = 2\pi/\lambda$, $k_{nx}$ is the projection of the wave vector of the coupled wave with the index $n$ onto the $ox$-axis, and $\|\varepsilon\|_{n-p}$ is the Toeplitz matrix [18] composed of the coefficients of the expansion of the dielectric constant in a complex Fourier series. The wave vector $k_{nx}$ is determined by the expression $k_{nx} = k_{0x} - 2\pi n/\Lambda$, where $k_{0x}$ is the projection of the wave vector onto the axis $ox$ of the zero-order Fourier component of the electromagnetic field, and $\Lambda$ is the grating period along the $ox$-axis.

The CWM equations for TM-polarization look like [14, 15, 18, 19]

$$\frac{dG_n(z)}{dz} = -ik_0 F_n(z) + i\frac{k_{nx}}{k_0} \sum_p \|\varepsilon\|_{n-p}^{-1} k_{px} F_p(z), \tag{3}$$

$$\frac{dF_n(z)}{dz} = -ik_0 \sum_p \left\|\frac{1}{\varepsilon}\right\|_{n-p}^{-1} G_p(z). \tag{4}$$

The system of differential equations (1) and (2) can be reduced to a system of equations of the second order, which – in the matrix form – is written down as

$$\frac{d^2\mathbf{G}(z)}{dz^2} = \mathbf{B}_e\mathbf{G}(z) = \mathbf{B}_1\mathbf{B}_2\mathbf{G}(z), \tag{5}$$

while, the corresponding equations (3) and (4) for TM-polarization can be written down as

$$\frac{d^2\mathbf{F}(z)}{dz^2} = \mathbf{B}_m\mathbf{F}(z) = \mathbf{B}_2\mathbf{B}_1\mathbf{F}(z), \tag{6}$$

where $\mathbf{B}_1$ and $\mathbf{B}_2$ are matrices which correspond to Eqs. (1) and (2) for TE-polarization and to Eqs. (3) and (4) for TM-one.

## 3. Equation Symmetry

In general case, the system of equations (5) and (6) is characterized by infinite dimensionality. However, in practice, calculations are carried out by taking into account a finite number of coupled waves. This number affects the accuracy of the analysis; but one has to bear in mind that making the dimensionality of the system of differential equations twice as large results in the increasing of computation time by a factor of about 8 [20].

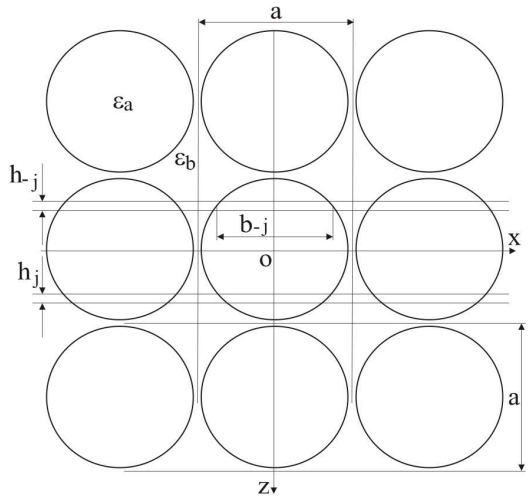


Fig. 1. 2D photonic crystal simulated as an infinite stack of gratings

Practically all 2D photonic crystals are spatially symmetric [16]; mathematically, this fact is expressed by the following dependences of the dielectric constant on the coordinates $x$ and $z$: $\varepsilon(x,z) = \varepsilon(-x,z) = \varepsilon(x,-z)$. One may hope that such a symmetry can be used in order to speed up computations [17].

Consider the matrices $\mathbf{B}_e$ and $\mathbf{B}_m$, provided that either of the two following conditions holds true:

$$\varepsilon_n = \varepsilon_{-n}, \quad k_{0x} = 0, \tag{7}$$

or

$$\varepsilon_n = \varepsilon_{-n}, \quad k_{0x} = \frac{\pi}{\Lambda}. \tag{8}$$

Condition (7) is fulfilled, when a beam falls onto a grating normally to it. In this case, an odd number of coupled waves, $N = 2N_1 + 1$, should be taken into account in calculations. The coupled wave, for which $k_x = 0$, propagates normally to the grating; it will be designated as $G_0$ ($F_0$). Accordingly, the first and the last component of vectors $\mathbf{G}(z)$ and $\mathbf{F}(z)$ will be designated as $G_{-N_1}$, $G_{N_1}$ and $F_{-N_1}$, $F_{N_1}$, respectively.

Condition (8) is obeyed, if $|k_{1x}| = k_{0x}$, i.e. – from the viewpoint of the lattice theory – if a beam

falls onto the grating at the first Bragg angle. In this case, it is expedient to consider an even number of waves, $N = 2N_1$, in calculations. The coupled wave, for which $k_{0x} = \pi/\Lambda$, will be designated as $G_0$ ($F_0$). Accordingly, the first and the last component of vectors $\mathbf{G}(z)$ and $\mathbf{F}(z)$ will be designated as $G_{-N_1+1}$, $G_{N_1}$ and $F_{-N_1+1}$, $F_{N_1}$, respectively. It is conditions (7) and (8) that are fulfilled at constructing the band structure of a photonic crystal in the framework of the CWM.

For one thing, we intend to change over from the system of equations (5) to two equivalent systems of differential equations, the orders of which are half as large (and analogously for system (6)). To build the first system of equations, we sum up the first and the last equation in system (5), the second and the last but one, and so on. As a result, we obtain a linear system of $N_1$ differential equations for new variables, where the matrix elements $b^+_{n,p}$ of the matrix $\mathbf{B}^+_e$ are related to the elements $b_{n,p}$ of the matrix $\mathbf{B}_e$ as follows:

$$b^+_{n,p} = b_{N_1+n,N_1+p} + b_{N_1-n+1,N_1+p}. \tag{9}$$

To build the second system of equations, we subtract the last equation in system (5) from the first one; the same operation is to be done with the second and the last but one equation, and so on. As a result, we obtain a linear system of $N_1$ differential equations for new variables, where the matrix elements $b^-_{n,p}$ of the matrix $\mathbf{B}^-_e$ are related to the elements $b_{n,p}$ of the matrix $\mathbf{B}_e$ as follows:

$$b^-_{n,p} = b_{N_1+n,N_1+p} - b_{N_1-n+1,N_1+p}. \tag{10}$$

Provided that the beam falls onto the grating normally and system (5) includes $2N_1+1$ equations, the consideration is the same as if the Bragg condition holds true. But, in this case, there is no corresponding pair member for $G_0$ ($F_0$). The relevant procedure for this case is described in work [17].

After summation, we obtain a linear system of $N_1+1$ differential equations for new variables, with the matrix elements $b^+_{n,p}$ of the matrix $\mathbf{B}^+_e$ being related to the elements $b_{n,p}$ of the matrix $\mathbf{B}_e$ as follows:

$$b^+_{1,p} = \frac{b_{N_1+1,2N_1+2-p}}{2} + \frac{b_{N_1+1,2N_1+2-p}}{2},$$

$$b^+_{n>1,p} = b_{N_1+2-n,N_1+2-p} + b_{N_1+2-n,N_1+p}. \tag{11}$$

After subtraction, the matrix elements $b^-_{n,p}$ of the matrix $\mathbf{B}^-_e$ are related to the elements $b_{n,p}$ of the matrix $\mathbf{B}_e$ as follows:

$$b^-_{1,p} = \frac{b_{N_1+1,2N_1+2-p}}{2} - \frac{b_{N_1+1,2N_1+2-p}}{2},$$

$$b^-_{n>1,p} = b_{N_1+2-n,N_1+2-p} - b_{N_1+2-n,N_1+p}. \tag{12}$$

From Eq. (12), it follows that the elements in the first row and the first column of the matrix $\mathbf{B}^-_e$ equal zero; whence, one can draw a conclusion that the additional system of differential equations includes $N_1$ equations.

## 4. Robust *R*-Algorithm

Let us split the intervals $[0, a/2]$ and $[0, -a/2]$ into $J$ layers (see Fig. 1). The thickness of the $j$-th layer is $h_j$. The number of layers depends on the form of the function $\varepsilon(x, z)$, so that the $z$-dependence for $\varepsilon(x, z)$ could be neglected and the product $\mathbf{B_1}^{(j)}\mathbf{B}_2^{(j)}$ could be considered constant within each layer. The thicknesses of the extreme layers ($h_J$ and $h_{-J}$) with a homogeneous dielectric constant are equal (in the case of a photonic crystal with a square elementary cell) to

$$h_J = a/2 - \sum_{j=1}^{J-1} h_j \simeq a/2 - R,$$

where $R$ is the cylinder radius.

A question arise: how can the parameters of rectangles, $h_j$ and $b_j$, be selected in order that the set of rectangles would best approximate a circle. In our opinion, rather a reasonable approximation is the following one:

$$h_j = R\left[\sin\frac{j\pi}{2J} - \sin\frac{(j-1)\pi}{2J}\right], \quad b_j = 2R\cos\frac{j\pi}{2J}.$$

In these expressions, $j$ varies from 1 to $J-1$. Application of these equations to the lower and upper semicircles allows the circle to be approximated by a polygon which is characterized by the central symmetry and has four symmetry axes. With the growth of $J$, the accuracy of circle approximation becomes evidently better. In the course of our calculations, the value of the parameter $R$ was made somewhat larger in order that the area of the approximation polygon be equal to that of the initial circle.

Having determined – for each layer – the eigenvalues $\gamma^2_{j,n}$ of the matrix $\mathbf{B}_1^{(j)}\mathbf{B}_2^{(j)}$ for TE-polarization ($\mathbf{B}_2^{(j)}\mathbf{B}_1^{(j)}$ for TM-one) and the corresponding eigenvectors, which

form the matrix $\mathbf{U}_j$, the solution of system (5) in the interval $[0, h_j]$ can be presented in the following form:

$$\mathbf{G}_j(z) = \exp(-\mathbf{A}_j z)\mathbf{C}_1^{(j)} +$$

$$+ \exp[-\mathbf{A}_j(h_j - z)]\mathbf{C}_2^{(j)}, \quad (13)$$

$$\mathbf{F}_j(z) = -\mathbf{Q}_j \exp(-\mathbf{A}_j z)\mathbf{C}_1^{(j)} +$$

$$+\mathbf{Q}_j \exp[-\mathbf{A}_j(h_j - z)]\mathbf{C}_2^{(j)}, \quad (14)$$

where the matrix $\mathbf{A}_j = \mathbf{U}_j\mathbf{\Gamma}_j\mathbf{U}_j^{-1}$; $\mathbf{\Gamma}_j$ is a diagonal matrix formed on the basis of the arranged sequence of numbers $\gamma_{j,n} = +\sqrt{\gamma_{j,n}^2}$; $\exp(-\mathbf{A}_j h_j) = \mathbf{U}_j \exp(-\mathbf{\Gamma}_j d_j)\mathbf{U}_j^{-1}$; $\mathbf{Q}_j = i\mathbf{A}_j/k_0$; and $\mathbf{C}_1^{(j)}$ and $\mathbf{C}_2^{(j)}$ are vectors which are determined by the boundary conditions at $z = 0$ and $z = h_j$. The solution of the system of equations (6) is expressed in a similar form. Within each layer, the coordinate $z$ varies either from 0 to $h_j$ for positive or from 0 to $-h_j$ for negative $z$, i.e. the local coordinate system is used.

In the robust R-algorithm, we express $\mathbf{C}_1^{(j)}$ and $\mathbf{C}_2^{(j)}$ – and, respectively, $\mathbf{F}_j(0)$ and $\mathbf{F}_j(h_j)$ – in terms of $\mathbf{G}_j(0)$ and $\mathbf{G}_j(h_j)$ in each local coordinate system. In the case of TM-polarized wave propagation, it is more expedient to express $\mathbf{G}_j(0)$ and $\mathbf{G}_j(h_j)$ in terms of $\mathbf{F}_j(0)$ and $\mathbf{F}_j(h_j)$, taking into account that the body of computations becomes smaller at that.

Hence, on the basis of Eqs. (13) and (14), we can write down the following expressions for waves with TE-polarization (for waves with TM-polarization, the expressions are analogous):

$$\mathbf{F}_j(0) = \mathbf{r}_1^{(j)}\mathbf{G}_j(0) + \mathbf{r}_2^{(j)}\mathbf{G}_j(h_j), \quad (15)$$

$$\mathbf{F}_j(h_j) = -\mathbf{r}_2^{(j)}\mathbf{G}_j(0) - \mathbf{r}_1^{(j)}\mathbf{G}_j(h_j), \quad (16)$$

where

$$\mathbf{r}_1^{(j)} = -\mathbf{Q}_j\mathbf{P}_2^{(j)} + \mathbf{Q}_j \exp(-\mathbf{A}_j h_j)\mathbf{P}_1^{(j)},$$

$$\mathbf{r}_2^{(j)} = -\mathbf{Q}_j\mathbf{P}_1^{(j)} + \mathbf{Q}_j \exp(-\mathbf{A}_j h_j)\mathbf{P}_2^{(j)}.$$

In their turn,

$$\mathbf{P}_1^{(j)} = -[\mathbf{I} - \exp(-2\mathbf{A}_j h_j)]^{-1} \exp(-\mathbf{A}_j h_j),$$

$$\mathbf{P}_2^{(j)} = [\mathbf{I} - \exp(-2\mathbf{A}_j h_j)]^{-1}.$$

Using the condition of equality between the tangential components of the electric and magnetic field strengths at the interface between layers $j$ and $j+1$, the quantities $\mathbf{G}_j(0)$, $\mathbf{G}_j(h_j)$, $\mathbf{F}_j(0)$, and $\mathbf{F}_j(h_j)$ must be excluded in sequence, and the quantities $\mathbf{F}_1(0)$ and $\mathbf{F}_J(h_J)$ must be expressed in terms of $\mathbf{G}_1(0)$ and $\mathbf{G}_J(h_J)$. For this purpose, we proceed from the first layer and determine $\mathbf{F}_1(0)$ and $\mathbf{F}_1(h_1)$ in terms of $\mathbf{G}_1(0)$ and $\mathbf{G}_1(h_1)$ as follows:

$$\mathbf{F}_1(0) = \mathbf{R}_{11}^{(1)}\mathbf{G}_1(0) + \mathbf{R}_{12}^{(1)}\mathbf{G}_1(h_1), \quad (17)$$

$$\mathbf{F}_1(h_1) = \mathbf{R}_{21}^{(1)}\mathbf{G}_1(0) + \mathbf{R}_{22}^{(1)}\mathbf{G}_1(h_1), \quad (18)$$

where $\mathbf{R}_{11}^{(1)} = \mathbf{r}_1^{(1)}$, $\mathbf{R}_{12}^{(1)} = \mathbf{r}_2^{(1)}$, $\mathbf{R}_{21}^{(1)} = -\mathbf{r}_2^{(1)}$, and $\mathbf{R}_{22}^{(1)} = -\mathbf{r}_1^{(1)}$. Taking the equality between the tangential components of the electric and magnetic field strengths at the interface between the first and the second layer, as well as relations (15), (16), (17), and (18), into account, we can express $\mathbf{F}_1(0)$ and $\mathbf{F}_2(h_2)$ in terms of $\mathbf{G}_1(0)$ and $\mathbf{G}_2(h_2)$ in the following manner:

$$\mathbf{F}_1(0) = \mathbf{R}_{11}^{(2)}\mathbf{G}_1(0) + \mathbf{R}_{12}^{(2)}\mathbf{G}_2(h_2), \quad (19)$$

$$\mathbf{F}_2(h_2) = \mathbf{R}_{21}^{(2)}\mathbf{G}_1(0) + \mathbf{R}_{22}^{(2)}\mathbf{G}_2(h_2), \quad (20)$$

where $\mathbf{R}_{11}^{(2)} = \mathbf{R}_{11}^{(1)} + \mathbf{R}_{12}^{(1)}\mathbf{D}_1^{(1)}$, $\mathbf{R}_{12}^{(2)} = \mathbf{R}_{12}^{(1)}\mathbf{D}_2^{(1)}$, $\mathbf{R}_{21}^{(2)} = -\mathbf{r}_2^{(2)}\mathbf{D}_1^{(1)}$, $\mathbf{R}_{22}^{(2)} = -\mathbf{r}_2^{(2)}\mathbf{D}_2^{(1)} - \mathbf{r}_1^{(1)}$, $\mathbf{D}_1^{(1)} = -[\mathbf{R}_{22}^{(1)} - \mathbf{r}_1^{(1)}]^{-1}\mathbf{R}_{21}^{(1)}$, and $\mathbf{D}_2^{(1)} = [\mathbf{R}_{22}^{(1)} - \mathbf{r}_1^{(1)}]^{-1}\mathbf{r}_2^{(2)}$. Considering the next layers by turn and making use of the method described above, we can ultimately express the quantities $\mathbf{F}_1(0)$ and $\mathbf{F}_J(h_J)$ in terms of $\mathbf{G}_1(0)$ and $\mathbf{G}_J(h_J)$ in the following form (here, the super- and subscripts are omitted):

$$\mathbf{F}(0) = \mathbf{R}_{11}\mathbf{G}(0) + \mathbf{R}_{12}\mathbf{G}(a_z/2), \quad (21)$$

$$\mathbf{F}(a_z/2) = \mathbf{R}_{21}\mathbf{G}(0) + \mathbf{R}_{22}\mathbf{G}(a_z/2). \quad (22)$$

From the analysis of the way used to obtain the $\mathbf{R}_{ms}^{(j)}$ matrices $(m, s = 1, 2)$ in accordance with expressions (15), (16), (19), and (20) and owing to the symmetry

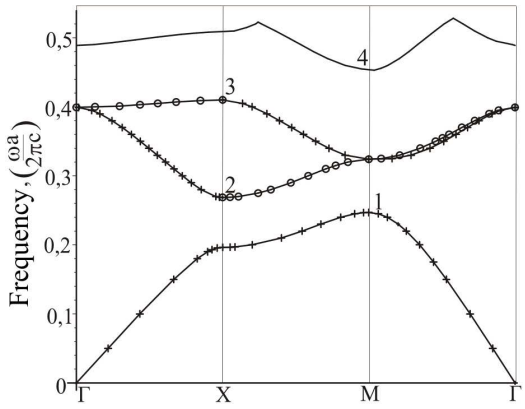


Fig. 2. Band structure of a photonic crystal with a square elementary cell (rods in air)

relation $\varepsilon(x,z) = \varepsilon(x,-z)$, a conclusion can be drawn that the following expressions are valid:

$$\mathbf{F}(0) = -\mathbf{R}_{11}\mathbf{G}(0) - \mathbf{R}_{12}\mathbf{G}(-a_z/2), \tag{23}$$

$$\mathbf{F}(-a_z/2) = -\mathbf{R}_{21}\mathbf{G}(0) - \mathbf{R}_{22}\mathbf{G}(-a_z/2), \tag{24}$$

with the matrices $\mathbf{R}_{ms}$ in expressions (21), (22), (23), and (24) being identical.

Having equated the right-hand sides in the systems of equations (21) and (23), we can express $\mathbf{G}(0)$ in terms of $\mathbf{G}(-a_z/2)$ and $\mathbf{G}(a_z/2)$, so that

$$\mathbf{G}(0) = -\frac{1}{2}\mathbf{R}_{11}^{-1}\mathbf{R}_{12}[\mathbf{G}(-a_z/2) + \mathbf{G}(a_z/2)]. \tag{25}$$

The next step comprises the substitution of Eq. (25) into systems of equations (22) and (24). Then, the final expressions read

$$\mathbf{F}(a_z/2) = -\frac{1}{2}\mathbf{R}_{21}\mathbf{R}_{11}^{-1}\mathbf{R}_{12}\mathbf{G}(-a_z/2) +$$

$$+[\mathbf{R}_{22} - \frac{1}{2}\mathbf{R}_{21}\mathbf{R}_{11}^{-1}\mathbf{R}_{12}]\mathbf{G}(a_z/2) =$$

$$= \mathbf{R}_1\mathbf{G}(-a_z/2) + \mathbf{R}_2\mathbf{G}(a_z/2),$$

$$\mathbf{F}(-a_z/2) = -[\mathbf{R}_{22} - \frac{1}{2}\mathbf{R}_{21}\mathbf{R}_{11}^{-1}\mathbf{R}_{12}] \times$$

$$\times\mathbf{G}(-a_z/2) + \frac{1}{2}\mathbf{R}_{21}\mathbf{R}_{11}^{-1}\mathbf{R}_{12}\mathbf{G}(a_z/2) =$$

$$= -\mathbf{R}_2\mathbf{G}(-a_z/2) - \mathbf{R}_1\mathbf{G}(a_z/2).$$

Accordingly, the eigenvalue and eigenvector problem [4, 14] looks like

$$\begin{pmatrix} \mathbf{0} & \mathbf{I} \\ \mathbf{R}_1 & \mathbf{R}_2 \end{pmatrix}\begin{pmatrix} \mathbf{G}(-a_z/2) \\ \mathbf{G}(a_z/2) \end{pmatrix} =$$

$$= \rho\begin{pmatrix} \mathbf{I} & \mathbf{0} \\ -\mathbf{R}_2 & -\mathbf{R}_1 \end{pmatrix}\begin{pmatrix} \mathbf{G}(-a_z/2) \\ \mathbf{G}(a_z/2) \end{pmatrix}, \tag{26}$$

where $\mathbf{0}$ is a square zero matrix, and $\mathbf{I}$ a unit diagonal matrix.

From the theory of photonic crystals [4], it follows that $\rho = \exp(ik_z a_z)$. Therefore, for an electromagnetic wave to freely propagate in a photonic crystal without damping, the parameter $k_z$ must be real-valued, i.e. the eigenvalues of problem (26) must be equal to unity by absolute value. In this case, the specific value of $k_z$ can be calculated by the expression

$$k_z = \arg(\rho)/a_z. \tag{27}$$

In order to construct the band structure of photonic crystals, it is necessary to vary the frequency of a propagating wave and, making use of expressions (26) and (27), to evaluate $k_z$ at fixed $k_x$ (equal to either 0 or $\pi/a_x$).

It is worth noting that, in expressions (21)–(27), we used the notation $a_z$, which corresponds to the period of the photonic crystal along the $oz$-axis; hence, in Fig. 1, $a_z = a$.

## 5. Numerical analysis of 2D photonic crystals

In Fig. 2, the band structure of a photonic crystal with a square elementary cell characterized by the parameters $\varepsilon_a = 8.9$, $\varepsilon_b = 1$, and $R = 0.38a$ is exhibited. Points $\Gamma$ $X$,, and $M$ are referred to as the points of high symmetry. On the way from point $\Gamma$ to point $X$, the wavevector component $k_x = 0$, while $k_z$ varies from 0 to $\pi/a$. Therefore, the elements of the symmetrized matrix can be determined by expressions (11) or (12). On the way from point $X$ to point $M$, $k_x = \pi/a$, while $k_z$ varies from 0 to $\pi/a$. So, we have another type of symmetry, and the elements of the symmetrized matrix are determined by expressions (9) and (10). On the way from point $M$ to point $\Gamma$, $k_x$ and $k_z$ vary synchronously from $\pi/a$ to zero. To calculate the band structure in this interval, we rotate the coordinate system by an angle of $\pi/4$ and superpose its origin with the cylinder center. In a new coordinate system, we select an elementary cell once more, but now its dimensions are different:

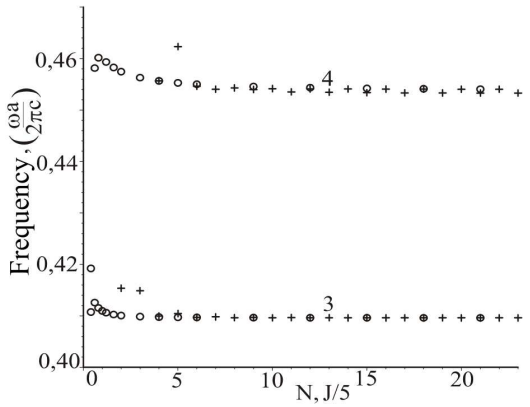


Fig. 3. Dependences of the calculated frequencies at high symmetry points on the number of diffraction orders $N$ taken into account (pluses, $J = 105$) and on the number of rectangles $J$ approximating the semicircle (circles, $N = 23$)

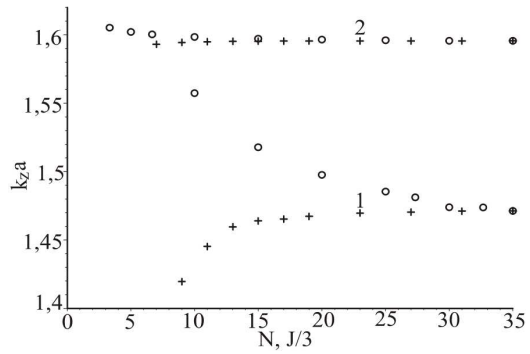


Fig. 4. Dependences of $k_z a$ on $N$ and $J$

$a_x = a_z = \sqrt{2}a$; now, in the new coordinate system, $k_x = 0$, and $k_z$ varies from $\sqrt{2}\pi/a$ to zero, i.e. the elements of the symmetrized matrix are determined by expressions (11) or (12).

In Fig. 2, in the branches of the band structure which contain points *1*, *2*, and *3*, one may discern pluses, which means that expressions (9) and (11) were used to calculate the corresponding sections of the branches, and circles, which means that expressions (10) and (12) were used. The corresponding modes are either symmetric (pluses) or antisymmetric (circles). However, at the high symmetry points, both the symmetric and antisymmetric modes with the same frequency can exist simultaneously; in this case, they are referred to as degenerate [4]. The calculation of this band structure was executed for $N = 23$ between points $\Gamma$ and $X$ and between points $M$ and $\Gamma$, and $N = 22$ between points $X$ and $M$; in this case, $J = 105$.

Point pairs (1,2) and (3,4) define the widths of two energy gaps. Therefore, it is of importance to determine the coordinates of those points, because they depend on $N$ and $J$. In Fig. 3, these dependences are plotted for points *3* and *4*.

The coordinates of points *3* and *4* were calculated for both $k_x = \pi/a$, i.e. $N$ was an even number, and $k_x = 0$, i.e. $N$ was an odd number. Here, it is of interest to find whether there is or there is not a frequency jump, when we approach the high symmetry points from the left and from the right. The frequency was calculated with an accuracy of five digits after the decimal point. One can see that, in order to obtain sufficiently exact results in this frequency range (from 0 to 0.47), the value for $N$ must be taken not less than 10, and that for $J$ larger than 50. For point *4*, a small frequency jump (in the fourth digit after the decimal point) is observed while approaching this point from the right and the left, which is practically unnoticeable in Fig. 2. This jump can be explained that the approximation cross-section of the rod is somewhat different in those two cases. If the parameter $J$ is increased to 200, the jump magnitude becomes substantially reduced.

It should be noted that the band structure depicted in Fig. 2 coincides – qualitatively and quantitatively – with that presented in Fig. 13 of Chapter 5 in monography [4].

In Fig. 4, we give the dependences of $k_z a$ on $N$ (pluses, $J = 105$) and $J$ (circles, $N = 35$) calculated for $k_x = 0$, $\varepsilon_a = 8.9$, $\varepsilon_b = 1$, $R = 0.38a$, and frequencies $\frac{\omega a}{2\pi c} = 0.5$ (points *1*) and 0.55 (points *2*). From this figure, it follows that, for point set *2*, i.e. for the frequency of 0.55, stable results can be obtained at $N = 11$ and $J = 50$; at the same time, for the frequency of 0.50, calculations have to be carried out at $N > 21$ and $J > 50$. Such a different sensitivity at different frequencies is governed by the derivative $d\omega/dk_z$: if this derivative is small, the sensitivity to $N$ and $J$ is high. Therefore, our calculations of the band structure were executed at $N \geq 21$ and $J \geq 50$.

In Fig. 5, the band structure of a 2D photonic crystal with a triangular elementary cell and the parameters $\varepsilon_a = 13$, $\varepsilon_b = 1$, and $R = 0.24a$ is shown. In the interval from point $\Gamma$ to point $M$, calculations were executed at $a_x = a$ and $a_z = \sqrt{3}a$; in this case, $k_x = 0$, while $k_z$ was varied from zero to $2\pi/(\sqrt{3}a)$. In order to built the band structure branches from point $M$ to point $\Gamma$ (intermediate point K), the coordinate axes must be rotated by an angle of $\pi/2$; so that, in a new coordinate system, $a_z = a$, $a_x = \sqrt{3}a$, $k_x = 0$, and $k_z$ varies from $2\pi/a$ to 0. Between points $M$ and $K$, $k_z$ varies from $2\pi/a$ to $4\pi/3a$, and, between points $K$ and $\Gamma$, from $4\pi/3a$ to 0.

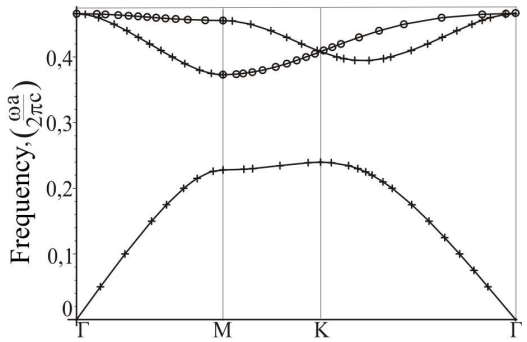


Fig. 5. Band structure of a 2D photonic crystal with a triangular elementary cell (cylindrical rods in air)

That is, while constructing the band structure of a photonic crystal with a triangular elementary cell, it is sufficient to use – at symmetrization – the rules according to expressions (11) and (12) – see pluses and circles, respectively, in the branches.

Making use of the method proposed, we also calculated the band structure of a photonic crystal with a triangular elementary cell and the parameters $\varepsilon_a = 1$, $\varepsilon_b = 13$, and $R = 0.48a$, i.e. for a system of regularly arranged holes in an insulator. According to our calculations, the ratio between the energy gap width and the medium band frequency is equal to 0.189 for $\varepsilon_b = 13$, which is in good agreement with the data of work [4], where the corresponding number was reported to be 0.186.

In the course of our calculations which demonstrated a new method by applying it to analyze the band structure of 2D photonic crystals, the values of dielectric constants taken from book [4] were used; the higher dielectric constant is close to the dielectric constant of GaAs (11.4 in the wavelength range 1–10 $\mu$m). The method proposed makes it possible to determine the allowed frequencies at arbitrary values of $\varepsilon_a$ and $\varepsilon_b$ and for an arbitrary structure of the elementary cell which can be characterized by definite periods along the $ox$- and $oz$-axes in a rectangular coordinate system.

It should be noted that the photonic forbidden energy gap can exist in such 2D photonic crystals, which are characterized by a large difference between the dielectric constants $\varepsilon_a$ and $\varepsilon_b$. In the case where $R = 0.48a$, $\varepsilon_a = 1$, and $\varepsilon_b < 6$, the energy gap is absent [12]. Therefore, 2D photonic crystals can be fabricated on the basis of chalcogenide glasses, the dielectric constant of which in the transparency range is higher than 6 [21]; the more so that the etching rate for such materials substantially varies at their illumination, and these materials are used in manufacturing relief holograms [22].

We also studied the dependence of the time of computation by the method proposed on $N$ at a fixed $J$, and on $J$ at a given $N$ for a photonic crystal with a square elementary cell. The computation time increases linearly with the increase of $J$; at the same time, it increases by a factor of approximately $2^3$, if $N$ becomes twice as large. These results coincide with the conclusions of work [20]. If $J = 256$ and $N = 32$, the value of the parameter $k_z$ can be determined – at fixed $\frac{\omega a}{2\pi c}$ and $k_x$ – within 115 conditional time units of computation (one conditional time unit is needed to determine eigenvalues and eigenvectors of expression (26), provided $N = 32$). Supposing that, at $N = 32$, the method proposed is equivalent to the plane-wave method, where the eigenvalues and eigenvectors of a matrix with dimensionality $2N^2 \times 2N^2 = 2048 \times 2048$ are to be found, the corresponding time of computation by the plane-wave method would amount to $(2N^2/N)^3 = 2^{18}$ standard units. Hence, the ratio between the computation times by the plane-wave and coupled-wave methods is equal to $2^{18}/115 > 2^{11} = 2048$. Therefore, the method proposed makes it possible to quickly determine whether the given frequency $\frac{\omega a}{2\pi c}$ is allowed to propagate in a photonic crystal at a definite value of $k_x$ and, accordingly, to calculate $k_z$. In the framework of our method, operations of matrix algebra are carried out for matrix dimensions much lower than those in the plane-wave method, which also brings about a higher accuracy of the analysis.

In addition, the method proposed has an extra advantage; namely, it is capable to determine at once whether the given frequency is allowed to propagate in a photonic crystal at a given $k_x$-value, which corresponds to practical needs in the course of developing the optical elements on the basis of 2D photonic crystals. In the framework of the plane-wave method, many numerical experiments are required to determine whether the given frequency is allowed or not at a fixed value of the component $k_x$.

## 6. Conclusions

A method proposed in work [14] to analyze the band structure of 2D photonic crystals (the coupled-wave method) has been developed further. A modified robust R-algorithm for numerical analysis of periodic structures was derived. Imposing the periodic boundary conditions gives rise to a necessity to solve an eigenvalue problem of the type $\mathbf{W_1 X} = \rho \mathbf{W_2 X}$ and to verify whether or not the absolute value of $\rho$ equals unity. If $|\rho| = 1$, the intended frequency is allowed. In general case, the

dimensionality of the vector $\mathbf{X}$ is equal to $2N$, two times the number of coupled waves used at the analysis. Owing to the spatial symmetry of the dielectric constant, a changeover can be made to the dimensionality $N\pm1$ or $N$ of the vector $\mathbf{X}$, without any loss of the analysis accuracy and with a simultaneous reduction of the computational time by a factor of about 8. The computational accuracy depends on the number of coupled waves $N$, which are taken into consideration, and the number $J$, which is defined as a number of rectangles needed to approximate the cross-section of the cylinder. With the growth of the frequencies of waves propagating in a photonic crystal, both $N$ and $J$ must be increased. The computational time increases almost linearly with growing $J$ and follows the cubic law with increasing $N$. The method proposed was applied to photonic crystals with a square or a triangular elementary cell, which are made up of cylindrical rods or include cylindrical holes. The further development of this coupled-wave method, which was created for 2D gratings, should include 3D photonic crystals into consideration, and a substantial gain in time and computation accuracy is expected.

The work was supported by the Foundation for Fundamental Researches of Ukraine (grant F25/602-2007).

1. I.A. Karachevceva, Semicond. Phys. Quant. Electr. Optoelectr. **7**, 430 (2004).
2. E. Yablonovitch, Phys. Rev. Lett. **58**, 2059 (1997).
3. E. Yablonovitch, T.J. Gmitter, and K.M. Leung, Phys. Rev. Lett. **67**, 2295 (1991).
4. J.D. Joannopoulis, R.D. Meade, and J.N. Winn, *Photonic Crystals: Molding the Flow of Light* (Princeton University Press, Princeton, 1995).
5. S. Foteinopoulou and C.M. Soukoulis, cond-mat/0212434 (unpublished).
6. U. Xu, J. Wang, Q. He *et al*, Opt. Express **13**, 5608 (2005).
7. N.A. Khizhnyak, Zh. Tekhn. Fiz. **27**, 2006 (1957).
8. E.A. Skirta and N.A. Khizhnyak, *Dispersion Properties of Artificial Anisotropic Insulators* (Institute of Radioelectronics, Academy of Sciences of the UkrSSR, Kharkiv, 1982) (in Russian).
9. N.A. Khizhnyak, *Integral Equations of Macroscopic Electrodynamics* (Kyiv, Naukova Dumka, 1986) (in Russian).
10. F. Seydon, O.M. Ramahi, R. Duraiswami, and T. Seppanen, Opt. Express **14**, 11362 (2006).
11. P. Dansas and N. Paraire, J. Opt. Soc. Am. A **15**, 1586 (1998).
12. A.E. Glushko, E.Ya. Glushko, and I.A. Karachevceva, Semicond. Phys. Quant. Electr. Optoelectr. **8**, 64 (2005).
13. H.S. Sozuer, J.W. Haus, and R. Inguva, Phys.Rev. B **45**, 13962 (1992).
14. V.M. Fitio, Ya.V. Bobitski, and G.P. Laba, Radiofiz. Elektron. **10**, 123 (2005).
15. M.G. Moharam, E.B. Grann, D.A. Pommet, and T.K. Gaylord, J. Opt. Soc. Am. A **12** 1068, (1995).
16. P.-G. Luan and Zh. Ye, cond-mat/0105428 (unpublished).
17. V.M. Fitio and Ya.V. Bobitski, Visn. Nats. Univ. Lviv. Politikhn. Ser. Elektron. N 513, 203 (2004).
18. V.M. Fitio and Ya.V. Bobitski, Opto-Electr. Rev. **13**, 331 (2005).
19. L. Li, J. Opt. Soc. Am. A **13**, 1870 (1996).
20. L. Li, J. Opt. Soc. Am. A **20**, 655 (2003).
21. I.Z. Indutnyi, M.T. Kostyshin, O.P. Kasyarum *et al.*, *Photoinduced Interactions in Metal–Semiconductor Structures* (Kyiv, Naukova Dumka, 1992) (in Russian).
22. V.I. Min'ko, I.Z. Indutnyy, P.F. Romanenko, and A.A. Kudryavtsev, Semicond. Phys. Quant. Electr. Optoelectr. **3**, 251 (2000).

Received 05.08.07.
Translated from Ukrainian by O.I. Voitenko

АНАЛІЗ ЗОННОЇ СТРУКТУРИ 2D ФОТОННИХ КРИСТАЛІВ МЕТОДОМ ЗВ'ЯЗАНИХ ХВИЛЬ: СТІЙКИЙ *R*-АЛГОРИТМ

*В.М. Фітьо, Я.В. Бобицький*

Р е з ю м е

Показано, що методом зв'язаних хвиль (МЗХ), який використовують для аналізу дифракції електромагнітних хвиль на плоских 1D-ґратках, при накладенні періодичних граничних умов можна швидко встановити, чи задана частота електромагнітної хвилі є дозволеною для поширення в 2D фотонному кристалі. Проблема зводиться до задачі на власні значення та власні вектори $\mathbf{W_1X} = \rho\mathbf{W_2X}$ і перевірки, чи власне число $\rho$ за модулем дорівнює одиниці. Якщо $|\rho| = 1$, то задана частота дозволена. Вимірність вектора $\mathbf{X}$ у розрахунку дорівнює подвоєному числу використаних зв'язаних хвиль $N \times 2$ і визначається необхідною точністю аналізу. Завдяки тому, що типові фотонні кристали мають симетричну просторову залежність діелектричної сталої, використання симетрії в залежності від її типу дозволяє перейти до вимірності вектора $\mathbf{X}$ $(N \pm 1)$ чи $N$ без втрати точності аналізу з одночасним зменшенням часу розрахунку приблизно у 8 разів. Для числового аналізу використано модифікований стійкий *R*-алгоритм.